CHALMERS

FINITE ELEMENT CENTER

PREPRINT 2003–26

A posteriori error estimation in computational inverse scattering

Larisa Beilina, Claes Johnson

Chalmers Finite Element Center
CHALMERS UNIVERSITY OF TECHNOLOGY
Göteborg Sweden 2003

CHALMERS FINITE ELEMENT CENTER

Preprint 2003–26

A posteriori error estimation in computational inverse scattering

Larisa Beilina, Claes Johnson

Chalmers Finite Element Center
Chalmers University of Technology
SE–412 96 Göteborg Sweden
Göteborg, December 2003

A posteriori error estimation in computational inverse scattering
Larisa Beilina, Claes Johnson
NO 2003–26
ISSN 1404–4382

Chalmers Finite Element Center
Chalmers University of Technology
SE–412 96 Göteborg
Sweden
Telephone: +46 (0)31 772 1000
Fax: +46 (0)31 772 3595
www.phi.chalmers.se

Printed in Sweden
Chalmers University of Technology
Göteborg, Sweden 2003

A POSTERIORI ERROR ESTIMATION IN COMPUTATIONAL INVERSE SCATTERING

LARISA BEILINA AND CLAES JOHNSON

Abstract. We present an adaptive finite element method for an inverse acoustic scattering problem, where the objective is to reconstruct an unknown wave speed coefficient inside a body from measured wave reflection data in time on parts of the surface of the body. The inverse problem is formulated as a problem of finding a zero of a Jacobian of a Lagrangian. The mesh in space is adaptively determined based on an a posteriori error estimate coupling residuals of the computed solution obtained by solving an associated linearized problem for the Hessian of the Lagrangian. The weights reflect the sensitivity of the reconstruction with respect to the discretization. We show concrete examples of reconstruction based on a posteriori error estimation.

1. Introduction

In this paper we consider an adaptive hybrid finite element/difference methods for an inverse scattering problem for a time-dependent scalar acoustic wave equation in the form of a parameter identification problem. The parameter represents the speed of wave propagation and occurs as a space-dependent coefficient in the wave equation, and the identification is made from partial knowledge of the solution of the wave equation in space and time. The objective is typically to determine the form and location of unknown objects (inhomogenities) inside a given surrounding body from measured wave reflection data in space and time on parts of the surface of the body. This problem arises in many applications including geophysics exploration, medical imaging and non-destructive testing.

The basic mathematical tool amounts to numerically solving the time-dependent acoustic wave equation with given wave speed coefficient, combined with least squares optimization to measured data, through which the wave speed coefficient with best wave reflection fit to the observed data, is determined. The optimality conditions, which express stationarity of an associated Lagrangian, involve a "forward" wave equation (state equation) and a "backward" wave equation (adjoint state equation), together with an equation expressing that the gradient with respect to the wave speed coefficient vanishes. The optimum is sought in an iterative process solving in each step the forward and backward wave equations

---

Date: 19th December 2003.

Larisa Beilina, Department of Mathematics, University of Basel, CH–4051 Basel, Switzerland, *email*: beilina@math.unibas.ch

Claes Johnson, Department of Mathematics, Chalmers University of Technology, S–412 96 Göteborg, Sweden, *email*: claes@math.chalmers.se.

and updating the material coefficients, in the form of a quasi-Newton method for the optimality equations.

The main purpose of this paper is to derive an a posteriori error estimate for the identification of the wave speed coefficient, and to present a couple of experiments showing the possibilities of computational inverse scattering using adaptive error control. The key ingredients of the a posteriori error estimate is evaluation of residuals relating to the Jacobian of the Lagrangian, combined with computation of stability factors/weights by solving an associated dual linearized problem involving the Hessian of the Lagrangian. We follow the main approach to adaptive error control in computational differential equations presented in [16] and [4] and related work.

In real applications the data is generated by emitting acoustic waves on the surface of the surrounding body, which penetrate the body and then are recorded on parts of the surface of the body. In the computational experiments of this note, instead synthetic data is generated by computing solutions of the wave equation with given wave speed coefficients and recording the corresponding solution on parts of the surface of the surrounding body. The objective is then to recover the wave speed coefficient inside the body from the recorded boundary data, normally with some noise added.

The reconstruction problem is "ill-posed" in the sense that quite different coefficients may correspond to very similar wave reflection data, and thus we need to "regularize" the reconstruction by introducing a regularizing term in the Lagrangian depending on a certain positive (small) coefficient γ, and it is important to choose γ adaptively to get a best reconstruction. If we choose γ too large, then we cannot match the measured data, while as γ gets smaller, the weights in the a posterori error estimate connected to the solution of the Hessian problem become larger, and again the reconstruction suffers. Balancing the two sources of error, we can adaptively determine a best value of γ. This value will depend on the quality of the measured data, with poor data typically demanding more regularization.

2. Acoustic wave propagation

The scalar wave equation modeling acoustic wave propagation in a bounded domain $\Omega \subset \mathbf{R}^d$, $d = 2, 3$, with boundary Γ, takes the following form:

$$
\begin{aligned}
\alpha \frac{\partial^2 p}{\partial t^2} - \triangle p = f, \qquad &\text{in } \Omega \times (0,T), \\
p(\cdot,0) = 0, \quad \frac{\partial p}{\partial t}(\cdot,0) = 0, \quad &\text{in } \Omega, \\
p\big|_{\Gamma} = 0, \quad &\text{on } \Gamma \times (0,T),
\end{aligned}
\tag{2.1}
$$

where $p(x,t) \in \mathbf{R}$ is the pressure satisfying homogeneous boundary and initial conditions, the coefficient $\alpha(x) = c(x)^{-2}$ with $c(x)$ the wave speed depending on $x \in \Omega$, t is the time variable and T is a final time, and $f(x,t)$ is a given source function. In the applications we also use different absorbing boundary conditions formulated to allow waves to leave the computational domain without reflections. The problem (2.1) is the forward problem with the coefficient $\alpha(x)$ being given and and we seek the solution $p(x,t)$. In the inverse problem, we seek $\alpha(x)$ from knowledge of $p(x,t)$ on parts of Γ.

2.1. **A hybrid finite element/difference method.** We use a hybrid finite element/difference method for time-domain acoustic/elastic wave propagation obtained by using continuous space-time piecewise linear finite elements on a partially structured mesh in space. The resulting scheme is efficiently implemented by (i) mass lumping in space and time making the scheme explicit in time and (ii) using a fixed finite difference stencil on the structured mesh.

The computational space domain Ω is decomposed into a finite element domain Ω_{FEM} with an unstructured mesh and a finite difference domain Ω_{FDM} with a structured mesh, with typically Ω_{FEM} covering only a small part of the Ω. In Ω_{FDM} we use quadraliteral elements in $\mathbf{R}^2$ and hexahedra in $\mathbf{R}^3$. In Ω_{FEM} we use a finite element mesh $K_h = \{K\}$ with elements K consisting of triangles in $\mathbf{R}^2$ and tetrahedra in $\mathbf{R}^3$). We associate with K_h a (continuous) mesh function $h = h(x)$ representing the diameter of the element K containing x. For the time discretization we let $J_\tau = \{J\}$ be a partition of the time interval $I = (0,T)$ into time intervals $J = (t_{k-1}, t_k]$ of uniform length $\tau = t_k - t_{k-1}$.

We define the following L_2 innner product and norm

$$((p,q)) = \int_\Omega \int_0^T pq \, dx \, dt, \quad \|p\|^2 = ((p,p)),$$

We further use the notation $Dv = \frac{\partial v}{\partial t}$.

To formulate a finite element method for (2.1) we introduce the finite element trial space W_h^p defined by:

$$W_h^p := \{w \in W^p : w|_{K\times J} \in P_1(K) \times P_1(J), \forall K \in K_h, \forall J \in J_\tau\},$$

where $P_1(K)$ and $P_1(J)$ denote the set of linear functions on K and J, respectively, and

$$W^p := \{w \in H^1(\Omega \times I) : w(\cdot, 0) = 0, w|_\Gamma = 0\}.$$

Correspondingly, we introduce the finite element test space W_h^φ defined by:

$$W_h^\varphi := \{w \in W^\varphi : w|_{K\times J} \in P_1(K) \times P_1(J), \forall K \in K_h, \forall J \in J_\tau\},$$

where

$$W^\varphi := \{w \in H^1(\Omega \times I) : w(\cdot, T) = 0, w|_\Gamma = 0\}.$$

In other words, the finite element spaces W_h^p and W_h^φ consist of continuous piecewise linear functions in space and time, satisfying certain homogeneous (initial) conditions at $t = 0$ and $t = T$. Note the abuse of notation here, where e.g. the index p in W_h^p signifies trial space in general, while it is also used to denote the exact solution in particular.

The finite element method for (2.1) now reads: Find $p_h \in W_h^p$ such that $\forall \bar\varphi \in W_h^\varphi$,

$$-((\alpha D p_h, D\bar\varphi)) + ((\nabla p_h, \nabla \bar\varphi)) = ((f^k, \bar\varphi)). \tag{2.2}$$

Here, the initial condition $Dp(0) = 0$ is imposed in weak form through the variational formulation.

2.2. **An explicit scheme for acoustic waves.** Expanding p in terms of the standard continuous piecewise linear functions in space and in time and substituting this into (2.2), the following system of linear equations is obtained:

$$
\begin{aligned}
M(\mathbf{p}^{k+1} - 2\mathbf{p}^k + \mathbf{p}^{k-1}) &= \\
\tau^2 F^k \quad - \quad & \tau^2 K(\frac{1}{6}\mathbf{p}^{k-1} + \frac{2}{3}\mathbf{p}^k + \frac{1}{6}\mathbf{p}^{k+1})
\end{aligned} \tag{2.3}
$$

with initial conditions $\mathbf{p}^0 = 0$, $\mathbf{p}^1 \approx 0$. Here, M is the mass matrix in space, K is the stiffness matrix for the Laplacian, F^k is the load vector at time level t_k corresponding to $f(\cdot,\cdot)$, and $\mathbf{p}^k$ denotes the vector of nodal values of $p(\cdot, t_k)$.

To obtain an explicit scheme we approximate M with the lumped mass matrix M^L, i.e., the diagonal approximation obtained by taking the row sum of M, see e.g. [19]. By multiplying (2.3) with $(M^L)^{-1}$ and replacing the terms $\frac{1}{6}\mathbf{p}^{k-1} + \frac{2}{3}\mathbf{p}^k + \frac{1}{6}\mathbf{p}^{k+1}$ by $\mathbf{p}^k$, we obtain the following efficient explicit method:

$$
\mathbf{p}^{k+1} \;=\; \tau^2 (M^L)^{-1} F^k + 2\mathbf{p}^k - \tau^2 (M^L)^{-1} K \mathbf{p}^k - \mathbf{p}^{k-1}. \tag{2.4}
$$

3. Inverse acoustic scattering

We formulate the inverse problem for acoustic scattering as an optimization problem where we seek the wave speed coefficient $c(x)$ which gives a wave equation solution with best least squares fit to time domain observations (measurements) at a finite set of observations points x_{obs}.

More precisely, our goal is to find the function $c(x)$ which minimizes the quantity

$$
E(p,c) = \frac{1}{2}\int_0^T \int_\Omega (p - \tilde{p})^2 \delta_{obs} dx dt + \frac{1}{2}\gamma \int_\Omega (|\nabla \alpha|^2 + \alpha^2) \;\; dx dt, \tag{3.1}
$$

where $\tilde{p}$ is observed data at x_{obs}, p satisfies (2.1) and thus depends on c, $\delta_{obs} = \sum \delta(x_{obs})$ is a sum of multiples of delta-functions $\delta(x_{obs})$ corresponding to the observation points, and γ is a regularization parameter.

To approach this minimization problem, we introduce the Lagrangian

$$
L(u) = E(p,c) - ((\alpha D p, D\varphi)) + ((\nabla p, \nabla \varphi)) - ((f, \varphi)),
$$

where $u = (p, \varphi, \alpha)$, and search for a stationary point with respect to u satisfying $\forall \bar{u}$

$$
L'(u; \bar{u}) = 0, \tag{3.2}
$$

where $L'(u;\cdot)$ is the Jacobian of L at u, and we assume that $\varphi(\cdot,T) = \bar{\varphi}(\cdot,T) = 0$ and $p(\cdot,0) = \bar{p}(\cdot,0) = 0$, together with homogeneous Dirichlet boundary conditions.

The equation (3.2) expresses that in $\Omega \times (0,T)$

$$\alpha \frac{\partial^2 p}{\partial t^2} - \triangle p = f, \tag{3.3}$$

$$\alpha \frac{\partial^2 \varphi}{\partial t^2} - \triangle \varphi = -(p-\tilde{p})\delta_{obs}, \tag{3.4}$$

$$-\gamma \triangle \alpha + \gamma \alpha - \int_0^T \frac{\partial p}{\partial t}\frac{\partial \varphi}{\partial t}\, dt = 0, \tag{3.5}$$

together with homogeneous boundary and initial conditions. The equation (3.3) is the state equation for the state p, the equation (3.4) is the adjoint state equation for the costate φ, and the equation (3.5) expresses stationarity with respect to the coefficient c.

3.1. **A finite element method for inverse acoustic scattering.** To formulate a finite element method for (3.2) we introduce the finite element space V_h of piecewise constants for the coefficient $c(x)$, defined by :

$$V_h := \{v \in L_2(\Omega) : v \in P_0(K), \forall K \in K_h\},$$

we recall the definition of W_h^p related to the state p and W_h^φ for the costate φ, and we define $U_h = W_h^p \times W_h^\varphi \times V_h$.

The finite element method for (3.2) now reads: Find $u_h \in U_h$, such that

$$L'(u_h; \bar{u}) = 0 \quad \forall \bar{u} \in U_h, \tag{3.6}$$

where the Laplacian regularization term is implemented using a discontinuous Galerkin method, see e.g. [10]. We solve this discrete problem using a quasi-Newton method with limited storage, with details of the implementation given in [9].

4. A posteriori error estimation for the Lagrangian

We obtain an a posteriori error estimate for error in the Lagrangian by first noting that

$$\begin{aligned} L(u) - L(u_h) &= \int_0^1 \frac{d}{d\epsilon} L(\epsilon u + (1-\epsilon)u_h) d\epsilon \\ &= \int_0^1 L'(\epsilon u + (1-\epsilon)u_h; u - u_h) d\epsilon \\ &= L'(u_h; u-u_h) + R, \end{aligned}$$

where R is a second order remainder term. Using next the Galerkin orthogonality (3.6) with a splitting $u - u_h = (u - u_h^I) + (u_h^I - u_h)$ where $u_h^I \in U_h$ denotes an interpolant of u, and neglecting the term R, we get the following error representation:

$$L(u) - L(u_h) \approx L'(u_h; u - u_h^I), \tag{4.1}$$

involving the residual $L'(u_h; \cdot)$ with $u - u_h^I$ appearing as a weight. We estimate $u - u_h^I$ in terms of derivatives of u and the mesh parameters h and τ, and we finally approximate the derivatives of u by corresponding derivatives of u_h. The a posteriori estimate (4.1) takes the following concrete form if we omit the γ-terms (for details, see [9]):

$$\begin{aligned} |L(u) - L(u_h)| \leq & \int_0^T \int_\Omega R_{p1}\sigma_\varphi \;\; dxdt + \int_0^T \int_\Omega R_{p2}\sigma_\varphi \;\; dxdt \\ + & \int_0^T \int_\Omega R_{p3}\sigma_\varphi \;\; dxdt + + \int_0^T \int_\Omega R_{\varphi 1}\sigma_p \;\; dxdt \\ + & \int_0^T \int_\Omega R_{\varphi 2}\sigma_p \;\; dxdt + \int_0^T \int_\Omega R_{\varphi 3}\sigma_p \;\; dxdt \\ + & \int_0^T \int_\Omega R_\alpha \sigma_\alpha \;\; dx \end{aligned} \tag{4.2}$$

where the different residuals R are defined as

$$\begin{aligned} R_{p_1} &= \big|f\big|, \;\; R_{p_2} = \max_{S\subset \partial K} \; h_k^{-1}\big|\big[\partial_s p_h\big]\big|, \;\; R_{p_3} = \alpha_h \tau^{-1}\big|\big[\partial_t p_h\big]\big|, \\ R_{\varphi_1} &= \big|p_h - \tilde{p}\big|, R_{\varphi_2} = \max_{S\subset \partial K} \; h_k^{-1}\big|\big[\partial_s \varphi_h\big]\big|, \;\; R_{\varphi_3} = \alpha_h \tau^{-1}\big|\big[\partial_t \varphi_h\big]\big|, \\ R_\alpha &= \left|\frac{\partial \varphi_h}{\partial t}\right| \cdot \left|\frac{\partial p_h}{\partial t}\right|, \end{aligned}$$

and the different weights σ have the following form:

$$\begin{aligned} \sigma_\varphi &= C_1 \tau \left|[\partial_t \varphi_h]\right| + C_1 h \left|[\partial_s \varphi_h]\right|, \\ \sigma_p &= C_1 \tau \left|[\partial_t p_h]\right| + C_1 h \left|[\partial_s p_h]\right|, \\ \sigma_\alpha &= C_2 \big|[\alpha_h]\big|, \end{aligned}$$

where $[v]$ on a space element K (or time-interval J) denotes the maximum of the modulus of the jump of the quantity v across a face of K (or boundary node of J), and in particular $[\partial_s v]$ on a space-element K denotes the maximum modulus of a jump in the normal derivative ov v across a side of K, and $[\partial_t v]$ on a time-interval J is the maxium modulus of the jump of the time derivative of v across a boundary node of J. Here $C_1 \sim 0.1$ and $C_2 \sim 1$ are interpolation constants.

5. An a posteriori error estimate for parameter identification

Now we present a more general a posteriori error estimate, which may be used to estimate the error in the parameter identification, our prime quantity of interest. This estimate involves the solution $\tilde{u}$ of the dual problem:

$$-L''(u_h; \bar{u}, \tilde{u}) = (\psi, \bar{u}) \;\; \forall \bar{u}, \tag{5.1}$$

where ψ acts as given data, and $L''(u; \cdot, \cdot)$ is the Hessian of the Lagrangian $L(u)$ at u, which expresses the sensitivity of the Jacobian $L'(u; \cdot)$ with respect to changes in u. Assuming this problem can be solved, we obtain choosing here $\bar{u} = u - u_h$ and using the fact that

$L''(u;\bar{u},\tilde{u})$ is symmetric in $\bar{u}$ and $\tilde{u}$, the following error representation:

$$\begin{aligned}((\psi, u-u_h)) &= -L''(u_h; u-u_h, \tilde{u})\\ &= -L'(u;\tilde{u}) + L'(u_h;\tilde{u}) + R\\ &= L'(u_h;\tilde{u}) + R = L'(u_h;\tilde{u}-\tilde{u}^I) + R,\end{aligned}$$

where $\tilde{u}^I$ is an interpolant of $\tilde{u}$ and again R is a second order remainder. Neglecting R we obtain the following analog of (4.1)

$$((\psi, u-u_h)) \approx L'(u_h;\tilde{u}-\tilde{u}^I),$$

with $\tilde{u}$ replacing u in the second argument. With proper choice of ψ and estimating $\tilde{u}-\tilde{u}^I$ as above by solving approximately for $\tilde{u}$, we may this way obtain, for example, an a posteriori error estimate for a mean value of the error in the parameter identification. The concrete form of this estimate is the same as that given above for the Lagrangian with only u replaced by $\tilde{u}$ in the weights.

Choosing different ψ as data in the dual problem, we obtain a posteriori control of the error in different quantities of interest. Below, we will typically choose $\psi = (0,0,1)$ in a domain containing the object, in which case the a posteriori error estimate gives control of a mean value of the coefficient α. We note that in the a posterori error estimate, the solution component $\tilde{\alpha}$ of the solution to the dual problem, or more precisely the jump $[\tilde{\alpha}]$ of a computed $\tilde{\alpha}$, appears as a weight in the equation expressing stationarity with respect to the coefficient α. We may thus view the jump $[\tilde{\alpha}]$ as a quantitative measure of a main aspect of sensitivity in the identification of α.

5.1. **The Hessian for the acoustic wave equation.** The Hessian $L''(u;\cdot,\cdot)$ of the Lagrangian $L(u)$ takes the form

$$\begin{aligned}L''(u;\bar{u},\tilde{u}) = &-((\alpha D\tilde{p}, D\bar{\varphi})) + ((\nabla\tilde{p},\nabla\bar{\varphi}))\\ &+ ((\bar{p},\tilde{p}))_{\delta_{obs}} - ((\bar{\alpha}D\tilde{p}, D\varphi))\\ &- ((\alpha D\bar{p}, D\tilde{\varphi})) + ((\nabla\bar{p},\nabla\tilde{\varphi})) - ((\bar{\alpha}Dp, D\tilde{\varphi}))\\ &- ((\tilde{\alpha}Dp, D\bar{\varphi})) - ((\tilde{\alpha}D\bar{p}, D\varphi)) + \gamma((\nabla\bar{\alpha},\nabla\tilde{\alpha})) + \gamma((\bar{\alpha},\tilde{\alpha}))\end{aligned}$$

and the dual problem thus takes the following strong form:

$$\begin{array}{rcl}\alpha D^2\tilde{\varphi} - \Delta\tilde{\varphi} + \tilde{p}_{\delta_{obs}} + D^2\varphi\tilde{\alpha} &=& \psi_1,\\ \alpha D^2\tilde{p} - \Delta\tilde{p} + D^2 p\tilde{\alpha} &=& \psi_2,\\ \displaystyle\int_0^T D^2\varphi\tilde{p}\;dt + \int_0^T \tilde{\varphi}D^2 p\;dt - \gamma\triangle\tilde{\alpha} + \gamma\tilde{\alpha} &=& \psi_3,\end{array} \tag{5.2}$$

together with initial and boundary conditions. The quantitative stability properties of this linear system in the form of estimation of the solution $\tilde{u}$ in terms of the data ψ, determines the sensitivity in the parameter identification to perturbations. Thus, we may say that the secret of parameter identification is reflected by the quantitative stability (or solvability) properties of the linear system (5.2), properties which can be determined by computational solution.

With correct data, the dual solution φ will be small and thus we may expect to be able to neglect the terms with $D^2\varphi$ as coefficient in (5.2). In this case one can directly prove uniqueness of the solution if $\gamma > 0$, which is a good sign, but the quantitative stability properties still remain to be evaluated. We may further expect the stability properties of this system to improve (the sensitivity to decrease), with increasing number of observation points and correct observations.

5.2. **An iterative method for solving the Hessian problem.** To solve the dual Hessian problem (5.2) with $u = (p, \alpha, \varphi)$ computed as above and the $D^2\varphi$ terms eliminated, we use the following iterative algorithm (where typically $\psi = (0, 0, 1)$ on some set including the object and zero else, corresponding to a mean value of the wave speed coefficient):

1. Choose an initial value $\tilde{u} = \tilde{u}^{old}$.
2. From the third equation in (5.2) update $\tilde{\alpha}$ according to

$$(1 + \rho\gamma)\tilde{\alpha}^{new} = \tilde{\alpha}^{old} + \rho(\psi_3 - \int_0^T \tilde{\varphi}^{old} D^2 p \, dt + \gamma \triangle \tilde{\alpha}^{old}) \tag{5.3}$$

3. From the second equation update $\tilde{p}$ by solving the wave equation

$$\alpha D^2 \tilde{p}^{new} - \Delta \tilde{p}^{new} = \psi_2 - D^2 p \tilde{\alpha}^{new} \tag{5.4}$$

4. From the first equation update $\tilde{\varphi}$ by solving the wave equation

$$\alpha D^2 \tilde{\varphi}^{new} - \Delta \tilde{\varphi}^{new} = \psi_1 - \tilde{p}^{new}_{\delta_{obs}} \tag{5.5}$$

5. Then set $\tilde{u}^{old} = \tilde{u}^{new}$ and go back to 2, and repeat until desired convergence is achieved.

Here, $\rho > 0$ is a step length at our choice.

As will be seen below, the Hessian problem is rather "ill-posed" in the sense that the value of the solution component $\tilde{\alpha}$ will be critically dependent on the regularization parameter γ, and in particular will increase as $\frac{1}{\gamma}$ as γ tends to zero. Luckily, as we noticed above, in the a posteriori error estimate the jump $[\tilde{\alpha}]$ appears rather than $\tilde{\alpha}$ itself (because of the Galerkin orthogonality), and the jump turns out to be less sensitive to the smallness of γ than $\tilde{\alpha}$ itself, and thus the error a posteriori estimation does not degenerate for small γ. Note that because of the normalization used, we will have to choose γ small (of the order 0.001 to 0.0001) in the inverse problem to not disturb the reconstruction by too much regularization. It is thus essential that the Hessian problem produces a solution component $\tilde{\alpha}$ with a jump that is not too large.

More precisely, keeping just the $\tilde{\alpha}$ terms the a posteriori error estimate for the coefficient α takes the form:

$$E_\alpha \equiv |(\alpha - \alpha_h, \psi_3)| \leq \int_0^T \int_\Omega \left| \frac{\partial \varphi_h(x,t)}{\partial t} \cdot \frac{\partial p_h(x,t)}{\partial t} \right| \cdot \left| [\tilde{\alpha}_h] \right| \; dxdt. \tag{5.6}$$

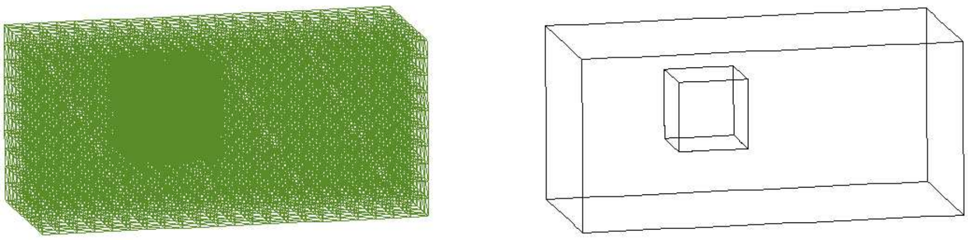

FIGURE 6.1. Cubic scatterer inside the finite element domain Ω_{FEM}

6. Numerical examples

We seek to identify a cubic scatter inside a computational domain $\Omega = [0, 5.0] \times [0, 2.5] \times [0, 2.5]$, which is split into a finite element domain $\Omega_{FEM} = [0.3, 4.7] \times [0.3, 2.3] \times [0.3, 2.3]$ with a nonstructured mesh, and a surrounding domain Ω_{FDM} with a structured mesh, see Fig. 6.1. We want to reconstruct the value of the coefficient α and we generate data corresponding to $\alpha = 2$ inside the cube, and $\alpha = 1$ in the rest of the domain. The space mesh in Ω_{FEM} consists of tetrahedra and in Ω_{FDM} of hexahedra with mesh size $h = 0.2$. We apply the method given above implemented as a hybrid finite element/difference method as presented in [8] with finite elements in Ω_{FEM} and finite differences in Ω_{FDM} with absorbing boundary conditions on the boundary of Ω. We generate pulses on top of Ω_{FEM} and record on the bottom of Ω_{FEM}, see Fig. 6.2.

We initiate six spherical pulses at the points $(0.45, 2.2, 1.25)$, $(1.25, 2.2, 1.25)$, $(2.05, 2.2, 1.25)$, $(2.95, 2.2, 1.25)$, $(3.75, 2.2, 1.25)$ and $(4.55, 2.2, 1.25)$, given by the source function

$$f_1(x, x_0) = \begin{cases} 10^3 \sin^2 \pi t & \text{if } 0 \le t \le 0.1 \text{ and } |x - x_0| < r, \\ 0 & \text{otherwise;} \end{cases} \tag{6.1}$$

In Fig. 6.2 we present the computed exact solution of the problem (2.1) inside Ω_{FEM}. The observation points are placed at the surface of the Ω_{FDM} on the opposite side to the initialization points. We use a total of 22 observation points. We perform tests with $T = 3.0$ and 300 time steps.

The optimization algorithm is started with an initial value of the parameter $\alpha = 1.0$ at all points of the computational domain. The computations was performed on five times adaptively refined meshes. In Table 1 we show computed L_2 norms of $p - p_{obs}$ on adaptively refined meshes with the regularization parameter $\gamma = 0.0001$. In Fig. 6.5 we present isosurfaces of the reconstructed parameter α on adaptively refined meshes.

In Fig. 6.3 we present the L_2 norms of $\tilde{\alpha}$ and $\tilde{\varphi}$ as functions of the number of iterations according to (5.3)-(5.5), computed with the regularization parameter $\gamma = 0.0001$ and $\rho = 100$. In Fig. 6.4 we present corresponding values of $\tilde{\alpha}$ at two different points.

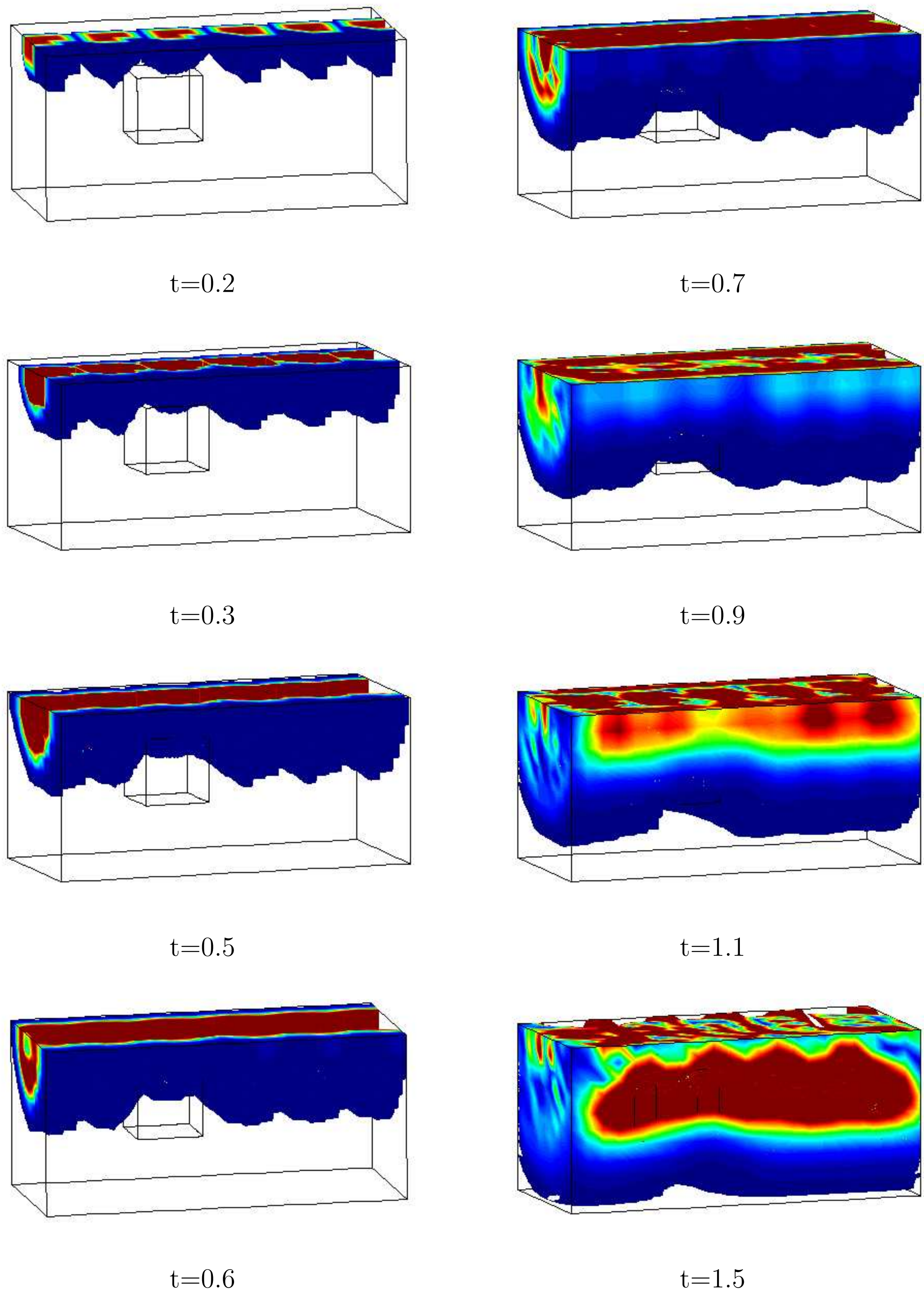

FIGURE 6.2. The exact solution displayed in Ω_{FEM}.

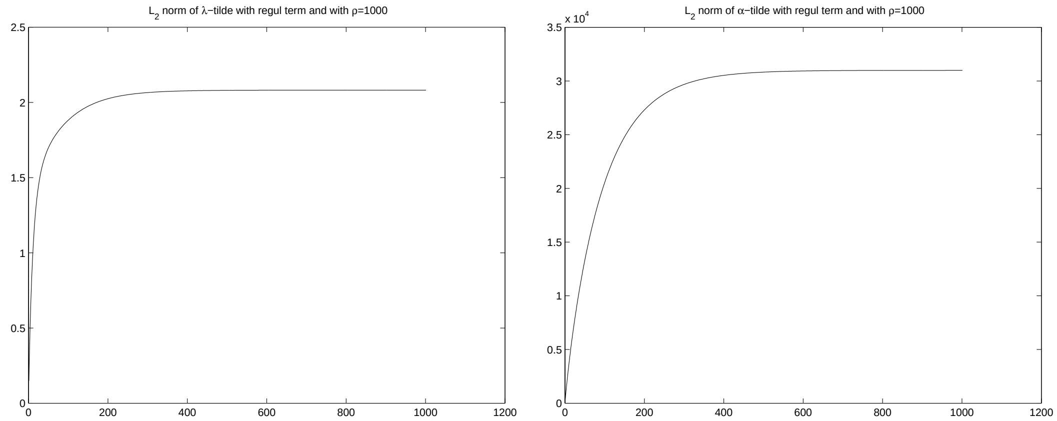

a) b)

FIGURE 6.3. In a) we display, in the case $\gamma = 0.0001$ and $\rho = 100$, the L_2 norm of $\tilde{\varphi}$ as a function of the number of iterations in the Hessian problem. The corresponding data for $\tilde{\alpha}$ is given in b). We notice that the norm of $\tilde{\alpha}$ is of the order $1/\gamma$, see also Fig 6.4.

.

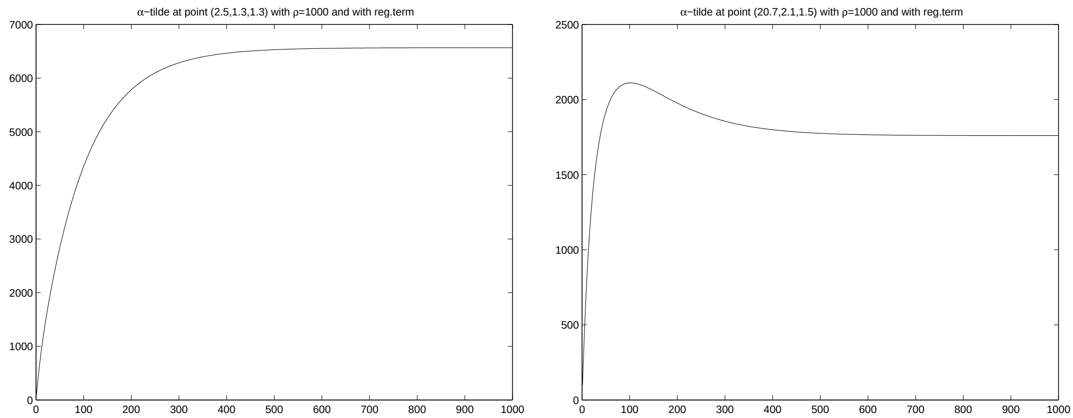

a) b)

FIGURE 6.4. In a) we display the value of $\tilde{\alpha}$ in the point (2.5,1.3,1.3) as a function of the number of iterations in the Hessain problem. The corresponding values at (0.7,2.1,1.5) are displayed in b). Again we have $\gamma = 0.0001$ and $\rho = 100$.

Evaluating the a posteriori error estimate (5.6) for the error E_α in the parameter α, we find $E_\alpha \leq 0.28$, which seems to be consistent with the level surface plots of Fig. 6.5. Again, notice that the jump $[\tilde{\alpha}]$ across inter-element edges of $\tilde{\alpha}$ occurs as a weight in the

opt.it.	2783 nodes	2847 nodes	3183 nodes	3771 nodes	4283 nodes	6613 nodes
1	0.0493302	0.0516122	0.051569	0.0529257	0.0535081	0.0537523
2	0.0405683	0.0423093	0.0419412	0.0428817	0.0433272	0.0439134
3	0.0235056	0.0239327	0.0245081	0.0271383	0.0285571	0.031920
4	0.0191902	0.0192185	0.0187792	0.0205331	0.0221997	0.0239426
5	0.0115005	0.0110448	0.0174202		0.0205711	0.0104240
6			0.0156732		0.0112331	0.0101503
7			0.0121359		0.0102246	

TABLE 1. The table presents the L_2 norm of computed $p - p_{obs}$ with $\gamma = 0.0001$ on different adaptively refined meshes and with 5 stored corrections in the quasi-Newton method.

a posteriori error estimate, not the value of $\tilde{\alpha}$ itself, and that the jump $[\tilde{\alpha}]$ is less sensitive to the smallness of the regularization parameter γ than $\tilde{\alpha}$ itself.

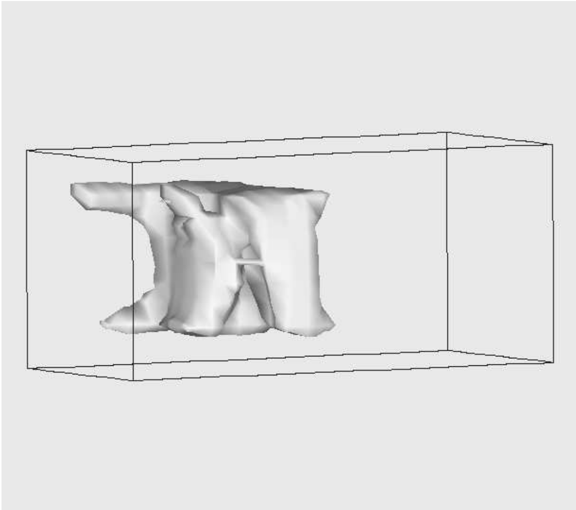

coarse mesh, 9 q.N. it., $\alpha \approx 1.21$

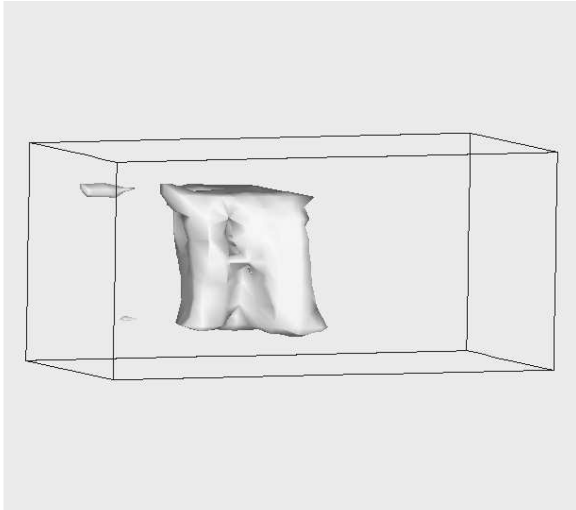

1 time ref., 8 q.N.it., $\alpha \approx 1.27$

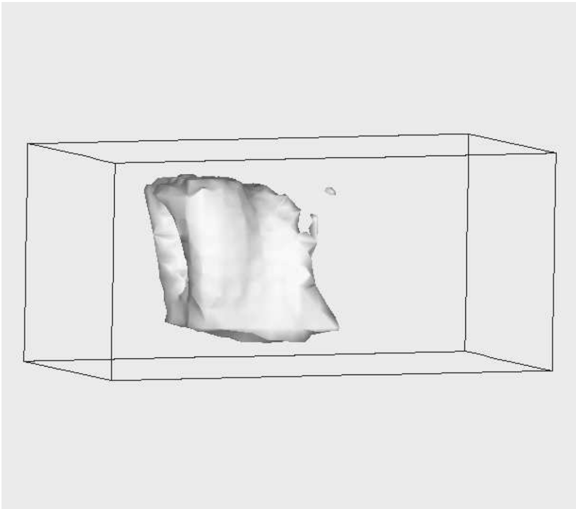

3 times ref.mesh, 4 q.N.it, $\alpha \approx 1.23$

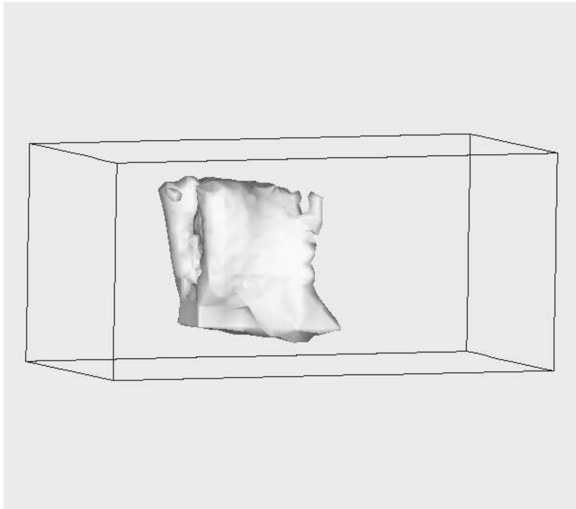

4 times ref.mesh, 9 q.N.it, $\alpha \approx 1.23$

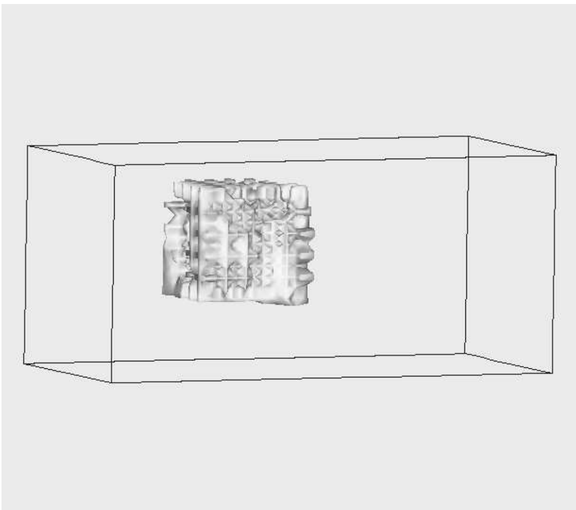

5 times ref.mesh, 8 q.N.it, $\alpha \approx 1.74$

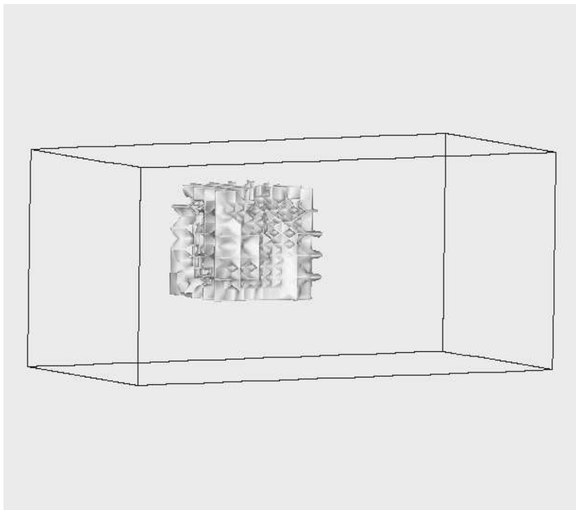

5 times ref.mesh, 9 q.N.it, $\alpha \approx 1.91$

FIGURE 6.5. The plots show level surfaces of the reconstructed parameter α on adaptively refined meshes with different number of quasi-Newton iterations (q.N.it) in the optimization.

References

[1] B. Auld, Acoustic fields and waves in solids Vol.2, ISBN 990090687X,Malabar,Krieger, 1990.

[2] E. Acklam, A. Jacobsen and H.P. Langtangen, Optimizing C++ code for explicit finite difference schemes, Oslo Scientific Computing Archive, Report 1998-4.

[3] S. Balay, W. Gropp, L-C. McInnes, B. Smith, PETSc user manual, http://www.mcs.anl.gov/petsc

[4] R. Becker, Adaptive finite elements for optimal control problems, Habilitationsschrift, Heidelberg, 2001.

[5] R. Becker, B. Vexler, Adaptive finite element methods for parameter identification problems, Preprint 2002-20 (SFB 359), Universität Heidelberg, 2002.

[6] R. Becker, R. Rannacher, An optimal control approach to a posteriori error estimation in finite element methods, In Acta Numerica 2001, Cambridge University Press, Cambridge, 2001.

[7] S. C. Brenner, L. R. Scott. The Mathematical theory of finite element methods, Springer-Verlag, 1994.

[8] L. Beilina, K. Samuelsson, K. Åhlander, A hybrid method for the wave equation. Proceedings of International Conference on Finite Element Methods, Gakuto International Series Mathematical Sciences and Applications, GAKKOTOSHO CO.,LTD, 2001.

[9] L. Beilina, Adaptive finite element method for an inverse scattering problem, J. Inverse Problems and Information Technologies, Vol.1, 2003.

[10] R. Bergström, M. Larson, Discontinuous/Continuous Least-Squares Finite Element Methods for Elliptic Problems, Chalmers Technical Report, 2002:11.

[11] J. Cea, A numerical method for the computation of an optimal domain, Lecture notes in computer sciences, Vol. 41, Springer, New York , 1976.

[12] G. C. Cohen, Higher Order numerical methods for transient wave equations, ISBN 3-540-41598-X, Springer Verlag Berlin Heidelberg New York, 2002.

[13] F. Edelvik, U. Andersson, and G. Ledfelt, Hybrid finite volume - finite difference solver for the Maxwell equations, In AP2000 Millennium Conference on Antennas & Propagation, Davos, Switzerland, 2000.

[14] B. Engquist, A. Majda, Absorbing boundary conditions for the numerical simulation of waves, Math. Comp., Volume 31, number 139, p.629–651, 1977.

[15] K. Eriksson, D. Estep and C. Johnson, Computational Differential Equations, Studentlitteratur, Lund, 1996.

[16] K. Eriksson, D. Estep and C. Johnson, Introduction to adaptive methods for differential equations, Acta Numerica 1995 (A.Iserles, ed.), pp. 105-158, Cambridge University Press, 1995.

[17] P. Hansbo, C. Johnson, Adaptive finite element methods for elastostatic contact problems, IMA Volumes in Mathematics and its Applications, 113, 135-150, 1998.

[18] J. Hoffman, C. Johnson, Dynamic computational subgrid modelling, Lecture Notes in Computational Science and Engineering, Springer, 2003.

[19] T. J. R. Hughes, The Finite Element Method, Prentice Hall, 1987.

[20] F. Ihlenburg, Finite Element Analysis of Acoustic Scattering, ISBN 0-387-98319-8, Springer-Verlag New York Berlin Heidelberg, 1998.

[21] C. Johnson, A. Szepessy, Adaptive finite element methods for conservation laws based on a posteriori error error estimation, Comm.Pure Appl.Math., 199-234, 1995.

[22] C. Johnson, Adaptive computational methods for differential equations, Proceedings from ICIAM99, eds Ball and Hunt, 96-104, Oxford University Press 2000.

Chalmers Finite Element Center Preprints

2001–01 *A simple nonconforming bilinear element for the elasticity problem*
Peter Hansbo and Mats G. Larson

2001–02 *The $\mathcal{LL}^*$ finite element method and multigrid for the magnetostatic problem*
Rickard Bergström, Mats G. Larson, and Klas Samuelsson

2001–03 *The Fokker-Planck operator as an asymptotic limit in anisotropic media*
Mohammad Asadzadeh

2001–04 *A posteriori error estimation of functionals in elliptic problems: experiments*
Mats G. Larson and A. Jonas Niklasson

2001–05 *A note on energy conservation for Hamiltonian systems using continuous time finite elements*
Peter Hansbo

2001–06 *Stationary level set method for modelling sharp interfaces in groundwater flow*
Nahidh Sharif and Nils-Erik Wiberg

2001–07 *Integration methods for the calculation of the magnetostatic field due to coils*
Marzia Fontana

2001–08 *Adaptive finite element computation of 3D magnetostatic problems in potential formulation*
Marzia Fontana

2001–09 *Multi-adaptive galerkin methods for ODEs I: theory & algorithms*
Anders Logg

2001–10 *Multi-adaptive galerkin methods for ODEs II: applications*
Anders Logg

2001–11 *Energy norm a posteriori error estimation for discontinuous Galerkin methods*
Roland Becker, Peter Hansbo, and Mats G. Larson

2001–12 *Analysis of a family of discontinuous Galerkin methods for elliptic problems: the one dimensional case*
Mats G. Larson and A. Jonas Niklasson

2001–13 *Analysis of a nonsymmetric discontinuous Galerkin method for elliptic problems: stability and energy error estimates*
Mats G. Larson and A. Jonas Niklasson

2001–14 *A hybrid method for the wave equation*
Larisa Beilina, Klas Samuelsson and Krister Åhlander

2001–15 *A finite element method for domain decomposition with non-matching grids*
Roland Becker, Peter Hansbo and Rolf Stenberg

2001–16 *Application of stable FEM-FDTD hybrid to scattering problems*
Thomas Rylander and Anders Bondeson

2001–17 *Eddy current computations using adaptive grids and edge elements*
Y. Q. Liu, A. Bondeson, R. Bergström, C. Johnson, M. G. Larson, and K. Samuelsson

2001–18 *Adaptive finite element methods for incompressible fluid flow*
Johan Hoffman and Claes Johnson

2001–19 *Dynamic subgrid modeling for time dependent convection–diffusion–reaction equations with fractal solutions*
Johan Hoffman

2001–20 *Topics in adaptive computational methods for differential equations*
Claes Johnson, Johan Hoffman and Anders Logg

2001–21 *An unfitted finite element method for elliptic interface problems*
Anita Hansbo and Peter Hansbo

2001–22 *A P^2–continuous, P^1–discontinuous finite element method for the Mindlin-Reissner plate model*
Peter Hansbo and Mats G. Larson

2002–01 *Approximation of time derivatives for parabolic equations in Banach space: constant time steps*
Yubin Yan

2002–02 *Approximation of time derivatives for parabolic equations in Banach space: variable time steps*
Yubin Yan

2002–03 *Stability of explicit-implicit hybrid time-stepping schemes for Maxwell's equations*
Thomas Rylander and Anders Bondeson

2002–04 *A computational study of transition to turbulence in shear flow*
Johan Hoffman and Claes Johnson

2002–05 *Adaptive hybrid FEM/FDM methods for inverse scattering problems*
Larisa Beilina

2002–06 *DOLFIN - Dynamic Object oriented Library for FINite element computation*
Johan Hoffman and Anders Logg

2002–07 *Explicit time-stepping for stiff ODEs*
Kenneth Eriksson, Claes Johnson and Anders Logg

2002–08 *Adaptive finite element methods for turbulent flow*
Johan Hoffman

2002–09 *Adaptive multiscale computational modeling of complex incompressible fluid flow*
Johan Hoffman and Claes Johnson

2002–10 *Least-squares finite element methods with applications in electromagnetics*
Rickard Bergström

2002–11 *Discontinuous/continuous least-squares finite element methods for elliptic problems*
Rickard Bergström and Mats G. Larson

2002–12 *Discontinuous least-squares finite element methods for the Div-Curl problem*
Rickard Bergström and Mats G. Larson

2002–13 *Object oriented implementation of a general finite element code*
Rickard Bergström

2002–14 *On adaptive strategies and error control in fracture mechanics*
Per Heintz and Klas Samuelsson

2002–15 *A unified stabilized method for Stokes' and Darcy's equations*
Erik Burman and Peter Hansbo

2002–16 *A finite element method on composite grids based on Nitsche's method*
Anita Hansbo, Peter Hansbo and Mats G. Larson

2002–17 *Edge stabilization for Galerkin approximations of convection–diffusion problems*
Erik Burman and Peter Hansbo

2002–18 *Adaptive strategies and error control for computing material forces in fracture mechanics*
Per Heintz, Fredrik Larsson, Peter Hansbo and Kenneth Runesson

2002–19 *A variable diffusion method for mesh smoothing*
J. Hermansson and P. Hansbo

2003–01 *A hybrid method for elastic waves*
L.Beilina

2003–02 *Application of the local nonobtuse tetrahedral refinement techniques near Fichera-like corners*
L.Beilina, S.Korotov and M. Křížek

2003–03 *Nitsche's method for coupling non-matching meshes in fluid-structure vibration problems*
Peter Hansbo and Joakim Hermansson

2003–04 *Crouzeix–Raviart and Raviart–Thomas elements for acoustic fluid–structure interaction*
Joakim Hermansson

2003–05 *Smoothing properties and approximation of time derivatives in multistep backward difference methods for linear parabolic equations*
Yubin Yan

2003–06 *Postprocessing the finite element method for semilinear parabolic problems*
Yubin Yan

2003–07 *The finite element method for a linear stochastic parabolic partial differential equation driven by additive noise*
Yubin Yan

2003–08 *A finite element method for a nonlinear stochastic parabolic equation*
Yubin Yan

2003–09 *A finite element method for the simulation of strong and weak discontinuities in elasticity*
Anita Hansbo and Peter Hansbo

2003–10 *Generalized Green's functions and the effective domain of influence*
Donald Estep, Michael Holst, and Mats G. Larson

2003–11 *Adaptive finite element/difference method for inverse elastic scattering waves*
L.Beilina

2003–12 *A Lagrange multiplier method for the finite element solution of elliptic domain decomposition problems using non-matching meshes*
Peter Hansbo, Carlo Lovadina, Ilaria Perugia, and Giancarlo Sangalli

2003–13 *A reduced P^1–discontinuous Galerkin method*
R. Becker, E. Burman, P. Hansbo, and M. G. Larson

2003–14 *Nitsche's method combined with space–time finite elements for ALE fluid–structure interaction problems*
Peter Hansbo, Joakim Hermansson, and Thomas Svedberg

2003–15 *Stabilized Crouzeix–Raviart element for the Darcy-Stokes problem*
Erik Burman and Peter Hansbo

2003–16 *Edge stabilization for the generalized Stokes problem: a continuous interior penalty method*
Erik Burman and Peter Hansbo

2003–17 *A conservative flux for the continuous Galerkin method based on discontinuous enrichment*
Mats G. Larson and A. Jonas Niklasson

2003–18 *CAD–to–CAE integration through automated model simplification and adaptive modelling*
K.Y. Lee, M.A. Price, C.G. Armstrong, M.G. Larson, and K. Samuelsson

2003–19 *Multi-adaptive time integration*
Anders Logg

2003–20 *Adaptive computational methods for parabolic problems*
Kenneth Eriksson, Claes Johnson, and Anders Logg

2003–21 *The FEniCS project*
T. Dupont, J. Hoffman, C. Johnson, R. Kirby, M. Larson, A. Logg, and R. Scott

2003–22 *Adaptive finite element methods for LES: Computation of the mean drag coefficient in a turbulent flow around a surface mounted cube using adaptive mesh refinement*
Johan Hoffman

2003–23 *Adaptive DNS/LES: a new agenda in CFD*
Johan Hoffman and Claes Johnson

2003–24 *Multiscale convergence and reiterated homogenization of parabolic problem*
Anders Holmbom, Nils Svanstedt, and Niklas Wellander

2003–25 *On the relationship between some weak compactnesses with different numbers of scales*
Anders Holmbom, Jeanette Silfver, Nils Svanstedt, and Niklas Wellander

2003–26 *A posteriori error estimation in computational inverse scattering*
Larisa Beilina and Claes Johnson

These preprints can be obtained from

`www.phi.chalmers.se/preprints`